Progress In Electromagnetics Research M, Vol. 60, 67–73, 2017

Experimental Studies of Passive Intermodulation in Metal-to-Metal Contacts

Gilles Duteil[1, *], Franck Colombel[1], Stephane Avrillon[1], Patrick Le Cam[2], and Jean P. Harel[2]

Abstract—This paper describes experimental studies of passive intermodulation due to metal-metal contacts. These studies cover the influence of roughness surface profile and of the thin native oxide layer on PIM value versus contact axial forces. A complete description of a dedicated test bench used during different studies is done. Moreover, obtained results are compared to observations published earlier.

1. INTRODUCTION

Passive intermodulation (PIM) products occur in passive devices when two or more signals mix together. In radio communication networks, PIM signals must be avoided as they may interfere with signals within reception frequency bands, degrading the quality of service. The intermodulation frequency F_{PIM}, resulting from two carriers, is described by:

$$F_{PIM} = mF_1 \pm nF_2 \tag{1}$$

where F_1 and F_2 are the two carrier frequencies, and $|m + n|$ provides the intermodulation order.

These unwanted mixes are created by nonlinearities that may be caused for example by dirty surfaces, loose connections, and poor soldering [1–3]. A small number of experimental studies on PIM level versus metal-metal contact have been published. [4] by Bayrak and Benson and [5] by Arazm and Benson are some of the most important of them. They have investigated the PIM from metal-metal contact in function of axial force and other numerous parameters such as roughness surface profile, different materials, different geometrical forms and cleanliness of surfaces. Nevertheless, the conditions of their studies do not comply with the 3rd Generation Partnership Project (3GPP) specification [6], which imposes a PIM measurement with carrier power at 43 dBm. More recent articles as [7, 8] have investigated PIM level in waveguide junctions. The main conclusion of these articles is that the PIM level from metal-metal contact is highly dependent on the cleanliness of the surface (e.g., thin oxide layers) and mechanical properties of contacting materials. According to [7], the main nonlinearities phenomenon in metal-metal contact is due to the tunneling effect, which appears in metal-oxide-metal regions (when metal materials are separated by thin oxide films).

This article describes different investigations on the metal-metal contact parameters impacting the passive intermodulation level in function of the axial force applied to a base station antenna context. In the first part, a complete description of the dedicated test bench manufactured to create a metal-metal contact and allowing the application of a controllable axial force is depicted. The second part focuses on investigations of PIM trend as a function of contact surface conditioning parameters such as roughness profile and presence of native oxide.

Received 28 June 2017, Accepted 25 August 2017, Scheduled 5 September 2017

* Corresponding author: Gilles Duteil (gilles.duteil@univ-rennes1.fr).

[1] Institute of Electronics and Telecommunications of Rennes, UMR CNRS 6164, University of Rennes 1, France. [2] Radio Frequency Systems, Lannion, France.

2. DESCRIPTION OF THE TEST BENCH

To investigate the PIM level in metal-metal contacts, a test setup made of an aluminum ground plane and two brass blocks, used to interface coaxial cables and stripline or suspended microstrip has been manufactured (Fig. 1). This kind of design is used for example in power divider in base station antenna. By this means, metal-metal contacts are created and localized between the ground plane and blocks. To reproduce a part of design used in base station antenna, an 83.2 mm length 50 Ω suspended microstrip line links the two brass blocks. This suspended microstrip line is made on Taconic TLX dielectric ($Dk = 2.55$ and $Df = 0.0012$ at 1.9 GHz) with a height of 0.8 mm. According to [9, 10], its use allows to reduce the influence of PIM sources from dielectric itself, such as PIM issues resulting from the copper cladding technics. Therefore, PIM sources from metal-metal contact are not disturbed by other PIM issues. Fig. 1 describes the test setup and provides the mechanical dimensions of it.

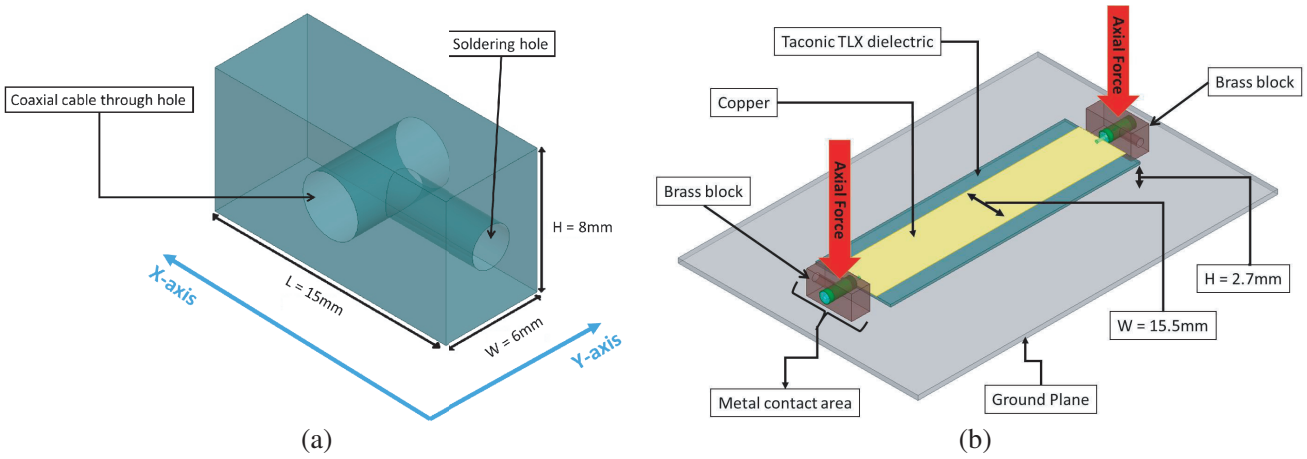

Figure 1. (a) Mechanical design of brass block. (b) Test setup synoptic.

Hydraulic cylinders are used to apply the axial force on brass blocks. According to Equation (2), the force (F in kN) created by hydraulic cylinders is linear dependent on the hydraulic pressure (ρ in bar) used and the hydraulic cylinder piston radius (R in cm).

$$\rho = \frac{100 \times F}{\pi \times R^2} \tag{2}$$

Hydraulic cylinders ($R = 2$ cm) and hydraulic pressure (from 0 to 60 bars) have been dimensioned to perform axial forces from 0 kN to 7.5 kN. By comparison, an M8 screw at 11 Nm tightening torque applies an axial force of 5.2 kN (i.e., international standard ISO-16047 [11]). To avoid any metallic contact between the hydraulic cylinder piston and the brass block, a ceramic interface has been inserted. Fig. 2 shows the return loss of the printed line connected to the 50 Ω cable through the brass block over a large bandwidth from 0.7 GHz to 1.2 GHz. The return loss for GSM band, from 910 MHz to 960 MHz, is less than −35 dB, by this way reducing the mismatching effect on PIM measurements as described in [12].

Reference [13] describes the synoptic of a PIM analyzer, taking into account that such a PIM analyzer is based on a standard PIM analyzer synoptic described in [6]. The PIM analyzer generates two carriers. These carriers are amplified by a high power amplifier. A combiner allows the carriers combination in the transmission path. A reflected IM duplexer and through IM duplexer are used to perform carriers cancellation, respectively in reflected IM measurement (backward measurement, i.e., reverse mode) and through IM measurement (forward measurement, i.e., forward mode). Described PIM measurements are completed with a PIM analyzer Kaelus SI-0900E [14] in GSM band. The PIM analyzer Kaelus SI-0900E generates two carriers ($F_1 = 935$ MHz and $F_2 = 960$ MHz) and, according to Equation (1), measures a third-order PIM level at 910 MHz. As the most used process measurements regarding base station antennas, all measurements presented in this article have been performed in backward (i.e., reverse mode).

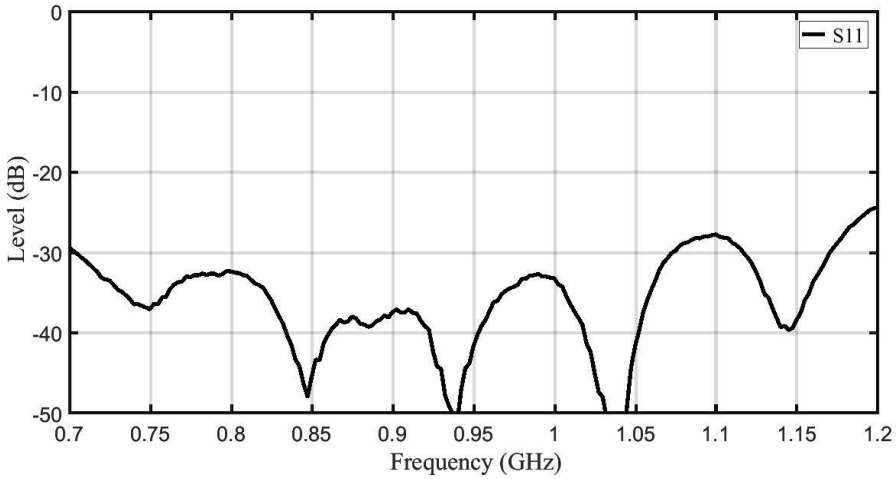

Figure 2. Test setup return loss measurement.

3. INVESTIGATIONS OF PIM LEVEL EVOLUTION VERSUS CONTACT SURFACE CONDITIONING

3.1. Surface Roughness Profile Influence

According to the roughness surface profile synoptic depicted in Fig. 3 and [15], the roughness of brass blocks can be defined by many parameters. The most common parameter R_a has been selected to define a surface profile. R_a represents the arithmetic mean deviation of measured profile, and it is defined by Equation (3).

$$R_a = \frac{1}{n}\sum_{i=1}^{n} |z_i| \tag{3}$$

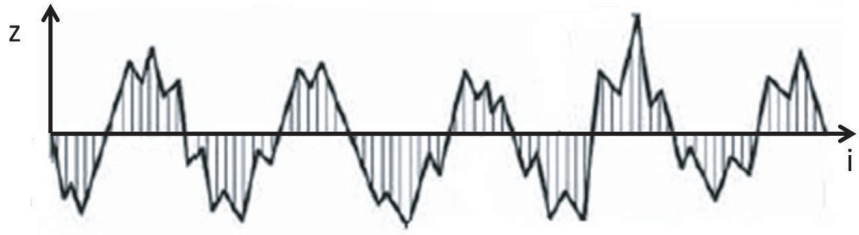

Figure 3. Roughness surface profile synoptic.

Table 1 provides R_a parameter measured from the two surfaces profile investigated in this article. R_a parameter of "Low Roughness profile" ranges from 0.2 µm to 0.3 µm along X-axis and from 0.2 µm to 0.25 µm along Y-axis while R_a of "High Roughness" profile ranges from 0.3 µm to 0.4 µm along X-axis and from 0.4 µm to 0.55 µm along Y-axis.

Table 1. R_a parameter for the two surfaces studied.

	R_a along X-axis (µm)	R_a along Y-axis (µm)
Low Roughness profile	[0.2–0.3]	[0.2–0.25]
High Roughness profile	[0.3–0.4]	[0.4–0.55]

Since the PIM level can be variable for identical test setups, for each surface profile, 10 test setups have been manufactured and measured. Using an axial force from 0.5 to 7 kN with a step of 0.5 kN, a complete campaign measurement for each surface profile represents 140 measurements. This solution permits to define a PIM trend for both roughness profiles. Fig. 4 plots the measured average and the 68% confidence interval of PIM level in function of the axial force for Low and High Roughness profiles, whereas Fig. 5 describes the standard deviation versus axial force of both roughness profiles. Observed results show two different trends of PIM level versus axial force as a function of roughness profile.

Figure 4 shows the first trend, for axial forces from 1 kN to 3 kN, wherein the average PIM level of high roughness profile is lower than the PIM level of low roughness profile. However, the 68% confidence intervals of both roughness profiles are crossed, on large part, each other. Taking into account this observation, it has been observed that PIM levels of high and low roughness profiles are statically closed for axial forces less than 3 kN. Nevertheless, according to Fig. 5, the standard deviations of both configurations are higher than 10 dB. This result shows a high variation of the PIM level independent of the roughness profile at low axial forces.

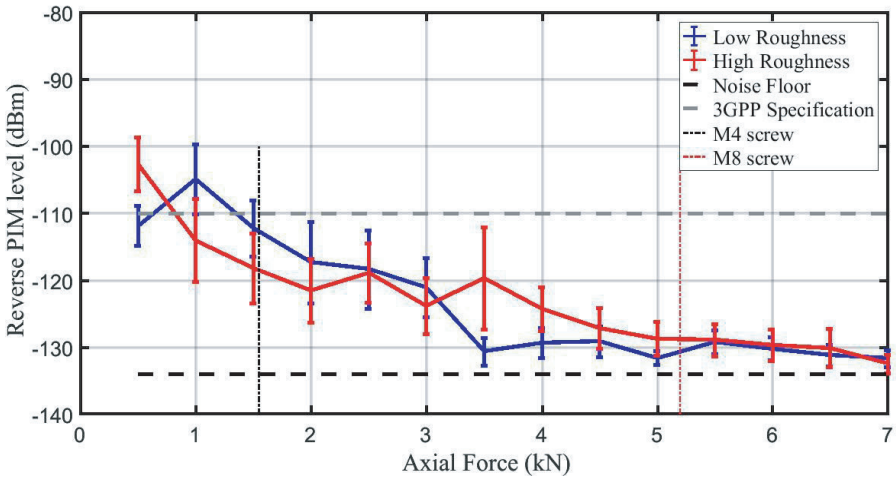

Figure 4. Comparison between "Low Roughness" and "High Roughness" surface profile average and 68% confidence interval of PIM measurements in function of axial force.

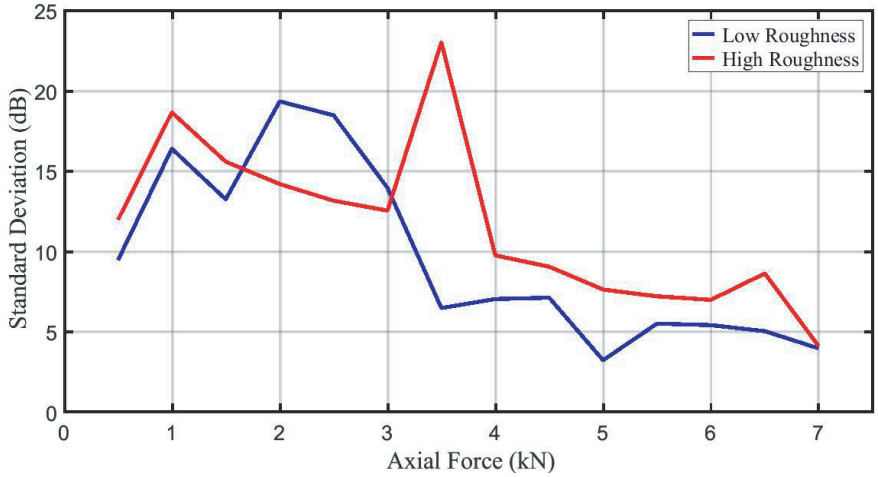

Figure 5. Comparison between "Low Roughness" and "High Roughness" surface profile standard deviation of PIM measurements in function of axial force.

According to Fig. 4, a second trend has been observed, for axial forces from 3.5 kN to 7 kN, wherein the low roughness average PIM level is lower than the PIM level of high roughness profile. It reaches −130 dBm starting from 3.5 kN, while average PIM level of high roughness profile reaches it from 5.5 kN. Moreover, for axial forces from 3.5 kN to 7 kN, Fig. 5 shows a low roughness standard deviation lower than the high roughness standard deviation. It means a better PIM level stabilization for low roughness setups at these axial forces. Despite a perturbed value at 3.5 kN for the high roughness profile, a −130 dBm PIM level stabilization has been observed at lower axial force for low profile roughness. This difference could be explained by the fact that rupture of oxide thin film requires lower axial force for low roughness profile than for high roughness profile. Therefore, the metal-oxide-metal area of low roughness profile is lower than the metal-oxide-metal of high roughness profile, which reduces the nonlinear influence of tunneling effect. Consequently, the PIM level of low roughness profile is lower than PIM level of high roughness profile.

3.2. Native Oxide Influence

Another measurement campaign has been performed with the aim of determining the influence of native oxide layer on PIM. Brass blocks (Fig. 1) have been gold plated with a 10 µm AuCo (99.75% of Au and 0.25% of Co) coat. Due to gold physical properties, it is admitted that no oxide layer appears on treated blocks. The roughness of coated blocks has been measured. Table 2 gives the R_a parameter for the gold plated blocks. It is observed that along X-axis, R_a values are higher than "High Roughness profile" while along Y-axis, R_a values are still approximatively the same as "High Roughness profile". Measured results show that only native oxide influence will be visualized.

Table 2. Measured gold plated R_a parameter along X and Y-axis.

	R_a along X-axis (µm)	R_a along Y-axis (µm)
Gold plated Roughness profile	[0.44–0.55]	[0.49–0.53]

The measurement campaign has been done with the same condition as previous measurements; 140 measurements of gold plated setup have been done. Comparison between gold plated and previous results shows a significant difference of average PIM level. According to Fig. 6, gold plated PIM level still decreases with increasing axial force as the previous measurement campaign. However, the average

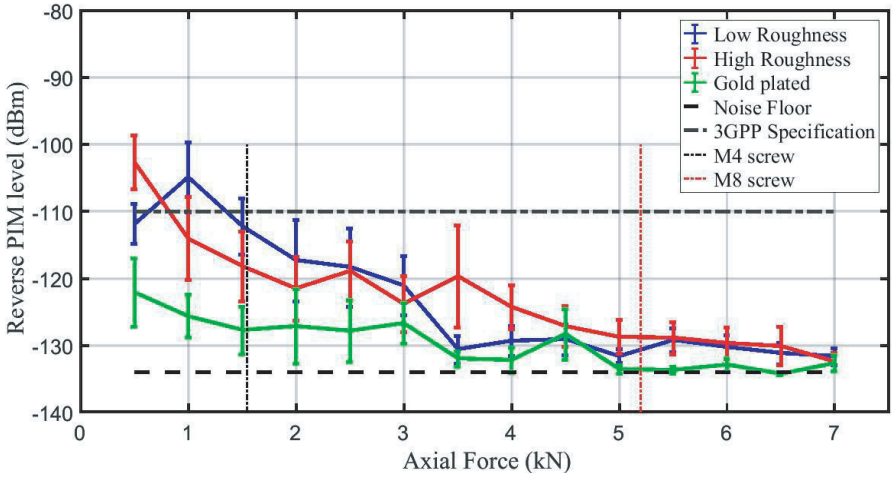

Figure 6. Comparison between Gold plated, "Low Roughness" and "High Roughness" surface profile average and 68% confidence interval of PIM measurements in function of axial force.

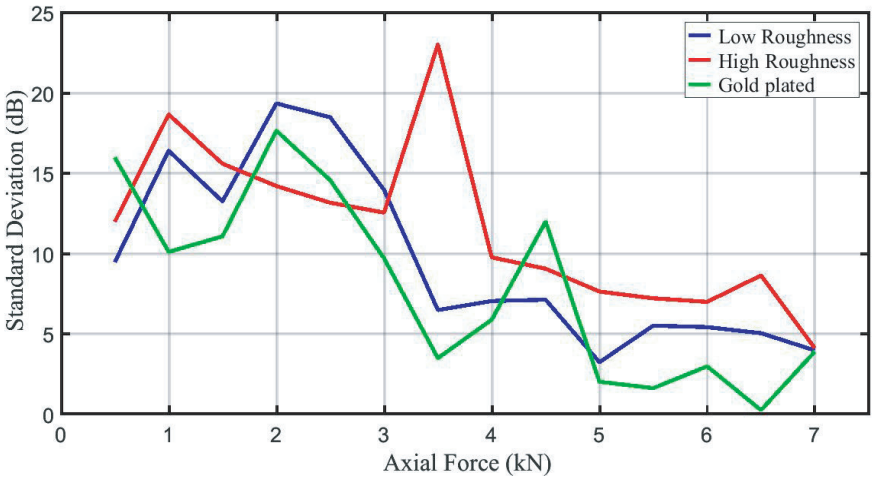

Figure 7. Comparison between Gold plated, "Low Roughness" and "High Roughness" surface profile standard deviation of PIM measurements in function of axial force.

PIM value of gold plated setup is below −120 dBm even at low axial force. According to Figs. 6 and 7, despite a perturbed measured value at 4.5 kN, PIM average reaches a level below −130 dBm from 3.5 kN despite R_a values higher than the Low Roughness values. For axial forces above 5 kN, no conclusion can be drawn as PIM level reaches the noise floor system. Very likely PIM level would still decrease. However, no PIM analyzer can at present perform measurement below −135 dBm and confirm this assumption. However, according to Fig. 7 and despite the defected value, it has been observed that gold plated setups have less fluctuation than Low and High Roughness. Observed results confirm a gold effect on passive intermodulation from metallic contact. Nevertheless, this effect can be either because no or less oxide layer induces a reduction of metal-oxide-metal area formation resulting in a decrease of nonlinear tunneling effect or because gold is mechanically softer than brass, resulting in metals contacts setting up requiring lower axial force.

4. CONCLUSION

In this paper, we have provided experimental results of passive intermodulation due to metallic contact versus different parameters. The metal-metal contact PIM level varies with the pressure applied to a brass block which is a common part of base station antenna. The results show a decrease and stabilization of PIM when axial force increases. It has been observed that the impact of axial force is different according to other contact parameters. Observed results of roughness influence investigation show a −130 dBm PIM level stabilization at lower axial force for low profile surfaces (3.5 kN) than high profile surfaces (5 kN). Moreover, to reduce and stabilize improve the PIM level, a surface treatment as the gold coating can be used. It has been observed that independent of roughness profile, gold-plated setup allows a lower and more stabilized PIM level, starting from −120 dBm to the noise floor PIM test bench level, than other tested setups despite low axial force. In a base station antenna context, the number of metallic contacts is numerous (higher than the two investigated in this paper). With the goal to have an antenna below the 3GPP specification, −110 dBm at 2×43 dBm, and using performed observations, a particular focusing must be done on:

- Using a surface coating, such as a gold plated treatment, on metallic contacts which drives high current density conduction.
- Reducing the surface roughness of metal parts in contact, to ease the stabilization of PIM level.
- Applying a specified axial force, in function of the contact area and parameters as roughness profile, permitting to reduce and stabilized PIM level from metal-metal contact.

ACKNOWLEDGMENT

The authors are grateful to Xavier Morvan, of Institute of Electronics and Telecommunications of Rennes, for his participation in designing and manufacturing the test bench described in this article.

REFERENCES

1. Lui, P. L., "Passive Intermodulation interference in communication systems," *Electron Electronics & Communication Engineering Journal*, Vol. 2, No. 3, 109–118, June 1990.
2. Best, G., "Passive Intermodulation (PIM) in broadcast transmission systems-lessons learned and a look into the future," *2014 IEEE International Symposium, Broadband Multimedia Systems and Broadcasting (BMSB)*, Jun. 25–27, 2014.
3. El Banna, B., T. Olsson, and J. Uddin, "Sources of passive intermodulation in base station antenna systems," *Proc. Antennas Propag. Conf.*, 139–144, Loughboroughl, U.K., 2006.
4. Bayrak, M. and F. A. Benson, "Intermodulation products from nonlinearities in transmission lines and connectors at microwave frequencies," *Proc. Inst. Elect. Eng.*, Vol. 122, No. 4, 361–367, Apr. 1975.
5. Arazm, F. and F. A. Benson, "Nonlinearities in metal contacts at microwave frequencies," *IEEE Trans. Electromagn. Compat.*, Vol. 3, 142–149, Aug. 1980.
6. *Passive Intermodulation (PIM) handling for Base Stations (BS)*, 3GPP TR 37.808, 2013.
7. Vincente, C. and H. L. Hartnagel, "Passive-Intermodulation analysis between rectangular waveguide flanges," *IEEE Trans. on Microwave Theory and Techniques*, Vol. 53, No. 8, Aug. 2005.
8. Vincente, C., D. Wolk, H. L. Hartnagel, B. Gimeno, V. E. Boria, and D. Raboso, "Experimental analysis of Passive Intermodulation at waveguide flange bolted connections," *IEEE Trans. on Microwave Theory and Techniques*, Vol. 55, No. 5, May 2007.
9. Schuchinsky, A. G., J. Francey, and V. F. Fusco, "Distributed sources of Passive Intermodulation on printed lines," *Proc. IEEE AP-S Int. Symp.*, 447–450, Jul. 2005.
10. Shitvov, A. P., T. Olsson, J. Francey, D. E. Zelenchuk, A. G. Schuchinsky, and B. El Banna, "Effects of interface conditions and long-term stability of passive intermodulation response in printed lines," *IET Microw. Antennas Propag.*, Vol. 5, No. 1, 68–76, Jan. 2011.
11. *Fasteners — Torque/clamp force testing*, ISO-16047, 2005.
12. Shitvov, A. P., D. E. Zelenchuk, A. G. Schuchinsky, and V. F. Fusco, "Passive intermodulation in printed lines: Effects of trace dimensions and substrate," *IET Microw. Antennas Propag.*, Vol. 3, No. 2, 260–268, Feb. 2009.
13. Hartman, R., "Measuring the Passive Intermodulation performance of RF cable assemblies," Kaelus, [Online], Available: http://www.kaelus.com/en/specials-folder/pdf-files/wp_performance_rf_cable_assemblies.
14. Kaelus E-series PIM Analyzers Datasheet [Online], Available: http://www.castlemicrowave.com/assets/Uploads/PDF/e-series-pdf.pdf.pdf.
15. *Geometrical Product Specifications (GPS) — Surface texture: Profile method — Terms, definitions and surface texture parameters*, ISO-4287, 1997.